



Preparation and characterization of $\text{Cu}_2\text{ZnSn}(\text{S},\text{Se})_4$ film by drop-coating of $\text{Cu}_2\text{ZnSnS}_4$ nanoink

Xiao-Gong Lv, Jing-Yu Wang, Cheng-Jun Zhu* , Zhi-Ping Wang

Received: 8 October 2015 / Revised: 4 December 2015 / Accepted: 31 May 2016 / Published online: 28 June 2016
© The Nonferrous Metals Society of China and Springer-Verlag Berlin Heidelberg 2016

Abstract In this work, a simple and facile one-pot oleylamine solvothermal synthetic method was developed to synthesize $\text{Cu}_2\text{ZnSnS}_4$ (CZTS) nanocrystals. And the $\text{Cu}_2\text{ZnSn}(\text{S},\text{Se})_4$ (CZTSSe) thin films were prepared by selenizing CZTS nanocrystals. The obtained CZTS nanocrystals and CZTSSe films were studied using X-ray diffraction (XRD), transmission electron microscopy (TEM), scanning electron microscopy (SEM), energy-dispersive X-ray spectroscopy (EDX), and ultraviolet–visible spectrophotometer (UV–Vis). TEM results show that the sphere-like CZTS nanoparticles with diameter between 12 and 35 nm are polydispersed. XRD studies indicate that the prepared CZTS nanocrystals form kesterite crystal structure, and the CZTSSe films with kesterite crystal structure are also obtained at the annealing temperatures of 500 and 550 °C. In particular after annealing at 500 °C for 20 min, the CZTSSe film exhibits a smooth, uniform, crack-free, and large-grained topography and possesses Cu-poor and Sn-rich composition. Moreover, it shows strong optical absorption from visible to near-infrared (IR) region, and its optical band gap (E_g) is found to be about 1.44 eV.

Keywords Thin films; Oleylamine solvothermal; Crystal structure; CZTS nanocrystals

1 Introduction

Earth-abundant copper–zinc–tin–chalcogenide semiconductors, CZTS and CZTSSe, have received increasing attention in recent years for photovoltaic applications due to their excellent material properties such as earth-abundance very low toxicity, a near-optimal direct band gap of about 1.5 eV, and a large absorption coefficient ($>1 \times 10^4 \text{ cm}^{-1}$) [1, 2]. CZTSSe solar cells were first reported in 1996, with 0.66 % power conversion efficiency for the initial vacuum-deposited devices. In 2008, devices efficiency of 6.70 % was enabled by the vacuum-based approaches followed by subsequent optimizations [3]. Recently, the CZTSSe solar cells fabricated by CZTS nanocrystals have also achieved total-area conversion efficiency of 7.20 % [4], and the conversion efficiency of solar cell based on CZTS has reached 9.15 % by subsequent optimizations [5]. At present, the highest conversion efficiency of 12.60 % is found in kesterite materials from a vacuum-free CZTS nanocrystals “ink” precursor using hydrazine [6]. Up to now, most work on CZTS based solar cells is focused on bulk thin films which are usually deposited on a desired substrate by sputtering [7, 8], thermal evaporation of elements [9], electrodeposition [10], spray pyrolysis [11], and hot injection [1, 4, 12], etc. However, these methods have some drawbacks such as expensive precursors, complicated apparatus, toxic byproducts evolved during their synthesis, and relatively complex experimental conditions such as high annealing temperature and high-vacuum systems.

Here it was present a facile one-pot oleylamine solvothermal synthetic route for the production of CZTS nanocrystals. The structure and morphology of the as-obtained CZTS nanocrystals were characterized. The phase

X.-G. Lv, J.-Y. Wang, C.-J. Zhu*, Z.-P. Wang
Key Laboratory of Semiconductor Photovoltaic Technology of Inner Mongolia Autonomous Region, School of Physical Science and Technology, Inner Mongolia University, Hohhot 010021, China
e-mail: cjzhu@imu.edu.cn; ndcjzhu@126.com

X.-G. Lv
Ordos Institute of Technology, Ordos 017000, China

structure, morphology, composition, and optical properties of the CZTSSe thin films fabricated by using CZTS nanocrystals were also presented.

2 Experimental

The CZTS nanocrystals were synthesized by one-pot oleylamine solvothermal synthetic route, and the CZTSSe thin films were prepared by selenization of CZTS nanocrystals. The typical synthesis of the CZTS nanocrystals proceeded as follows: $\text{Cu}(\text{acac})_2$, namely cupric(II) acetylacetonate (1.50 mmol), $\text{Zn}(\text{acac})_2$, namely zinc(II) acetylacetonate (0.75 mmol), $\text{SnCl}_2 \cdot \text{H}_2\text{O}$ (0.75 mmol), and S powder (3.00 mmol) were mixed with 15.50 ml oleylamine under an inert atmosphere in a autoclave. The mixture was subsequently stirred in a suitable pressure and heated to 110 °C, reacted for 30 min at this temperature. The temperature was then increased to 280 °C and kept constant for 60 min for the mixture to fully react, allowing the nanoparticles to grow. After the reaction, the solution was rapidly cooled down to room temperature. At 60 °C, 10–15 ml solvent (hexane/ethanol volume ratio = 1:1) was added to the reaction mixture to prevent its solidification. The dispersed solution was washed repeatedly using hexane/isopropanol (volume ratio of 1:2) by a centrifuge. The collected CZTS nanocrystal precipitates were dried under an argon flow and dispersed in hexanethiol before being sonicated using ultrasound processor to form a stable CZTS nanoink with a concentration of approximate $80 \text{ mg} \cdot \text{ml}^{-1}$. The CZTS nanoink was drop-casted directly onto soda lime glass substrates and dried at moderate temperature in air for 12 h in order to form the CZTS precursor film. In drop-casting process, several CZTS nanoink drops covered the soda lime glass substrates, where the nanoparticles normally accumulated by self-assembling during the hexanethiol solvent evaporation. Subsequently, the CZTS precursor films were fabricated into CZTSSe films by annealing under Se vapor at mild conditions (350–550 °C for 20 min).

The phase structures of the products were analyzed using X-ray diffractometer (XRD, Empyrean, $\text{Cu K}\alpha$ radiation). The particle size and morphology of the products were investigated by transmission electron microscopy (TEM, FEI Tecnai F20) and scanning electron microscopy (SEM, Hitachi S-4800). The compositions of the CZTSSe thin films were determined by energy-dispersive X-ray spectroscopy (EDX, 11,280-47,470). The optical properties of the films were evaluated by ultraviolet–visible spectroscopy (UV–Vis, Lambda 750, PerkinElmer).

3 Results and discussion

3.1 Characterization of TEM for CZTS nanocrystals

Figure 1 shows TEM images of CZTS nanocrystals obtained after 60 min of reaction at 280 °C. As shown, the CZTS nanocrystals are polydispersed with particle sizes in the range of 12–35 nm (Fig. 1a–c). Despite the non-uniformity in their shape and size, the morphology of CZTS nanocrystals is mostly spherical (Fig. 1c). The individual nanocrystals are highly crystalline as shown in the high-resolution TEM (HRTEM) image (Fig. 1d). The measured interplane d -spacing of $\sim 0.31 \text{ nm}$ corresponds to the (112) lattice plane of tetragonal (kesterite) CZTS.

3.2 XRD result

Figure 2 shows XRD patterns of CZTS nanocrystals and CZTSSe thin films. The stick pattern of kesterite (tetragonal) CZTS (JCPDS No. 26-0575) is provided for reference. XRD pattern in Fig. 2a confirms that the CZTS nanocrystals form kesterite crystal structure and that there are no characteristic peaks of other binary sulfide impurities (ZnS , Cu_xS). The average grain size calculated from the full width at half maximum of (112) diffraction peak by Debye–Scherrer's formula is about 15 nm, which agrees well with the grain size obtained from TEM images. Figure 2b shows XRD patterns of the CZTSSe films fabricated by CZTS nanocrystals annealed at 350–550 °C. Despite containing Cu_xS impure phase in the films sintered at 350–450 °C, the major XRD peaks from (112), (220), and (312) planes of the films are visible, suggesting that the films have largely formed the kesterite structure. With the further increase in annealing temperature up to 500 °C, the Cu_xS phase disappears and the CZTSSe film has polycrystalline nature with single-phase kesterite crystal structures that are tetragonal systems, which can be confirmed by JCPDF No. 26-0575. And with increase in annealing temperatures, the diffraction peaks slightly shift to lower 2θ position, which can be attributed to the partial substitution of Se ion with larger size (0.198 nm) for S ion with smaller size (0.184 nm) [13].

3.3 Surface morphology

The surface morphologies of the selenized CZTSSe films at 350–500 °C are shown in Fig. 3. Films annealed at 350 and 400 °C (Fig. 3a, b) show a surface with voids and cracks probably due to low annealing temperature. The sample annealed at 450 °C (Fig. 3c) exhibits relatively regular morphology and some visible small grains, which may indicate incomplete recrystallization of the film. The CZTSSe film treated at 500 °C (Fig. 3d) exhibits a smooth,

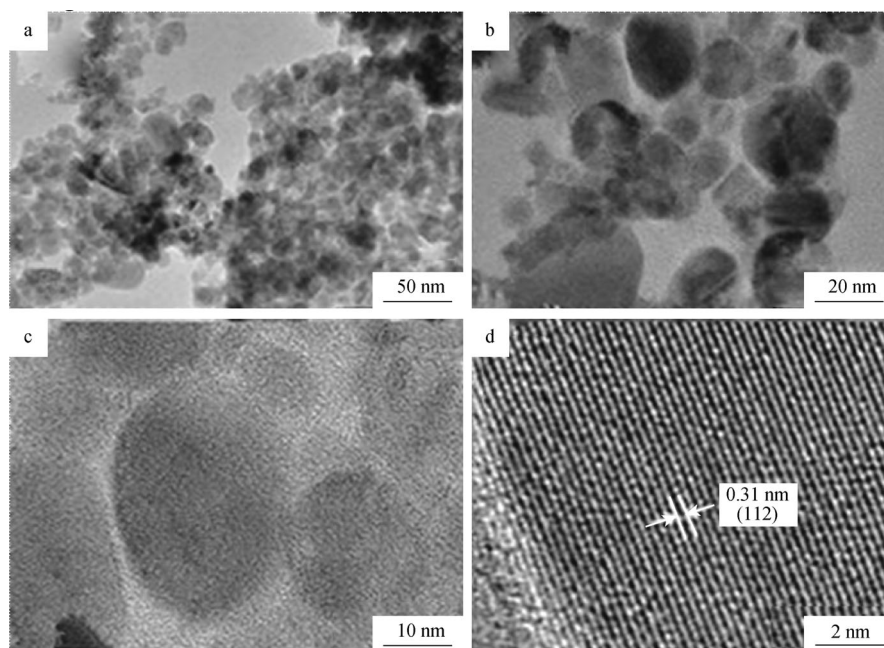


Fig. 1 Microstructures of CZTS nanocrystals: **a, b** TEM images and **c, d** HRTEM images

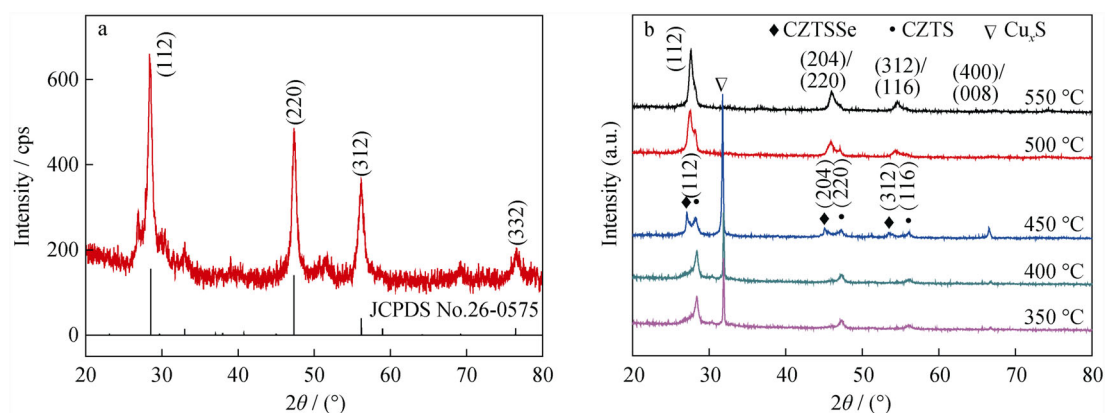


Fig. 2 XRD patterns of **a** prepared CZTS nanoparticles and **b** CZTSSe films annealed at 350–550 °C

uniform, and crack-free topography with relatively larger grains. And it can be seen that the CZTSSe film annealed at 500 °C exhibits strong adhesion to the glass substrate from the cross-sectional image of CZTSSe film in Fig. 4. However, the film annealed at 550 °C (Fig. 3e) has a few grains and pinholes, which is disadvantageous as absorber of solar cells.

3.4 Composition analysis

Figure 5 shows the relationship between elemental composition of CZTSSe films measured by EDX and post-annealing temperature. The composition of Se increases at the beginning and then decreases slightly. On the other

hand, the composition of S decreases first and then increases with annealing temperature increasing. This suggests that high selenization temperature is beneficial to the replacement of S by Se. It is also consistent with the result of previous reports [13, 14]. The atomic ratios of elemental compositions of CZTSSe films annealed at 350–550 °C are summarized in Table 1. The atomic ratios of Cu/(Zn + Sn) for films annealed at 350, 400, 450, 500 and 550 °C are 0.82, 0.88, 0.86, 0.96 and 0.72, respectively, and those of (Zn/Sn) are 0.70, 0.71, 0.38, 0.51 and 0.66 for the corresponding temperatures. XRD results indicate that the layers have a single-phase kesterite structure for CZTSSe annealed at 500 and 550 °C, as shown in Fig. 2. However, for those annealed at 550 °C,

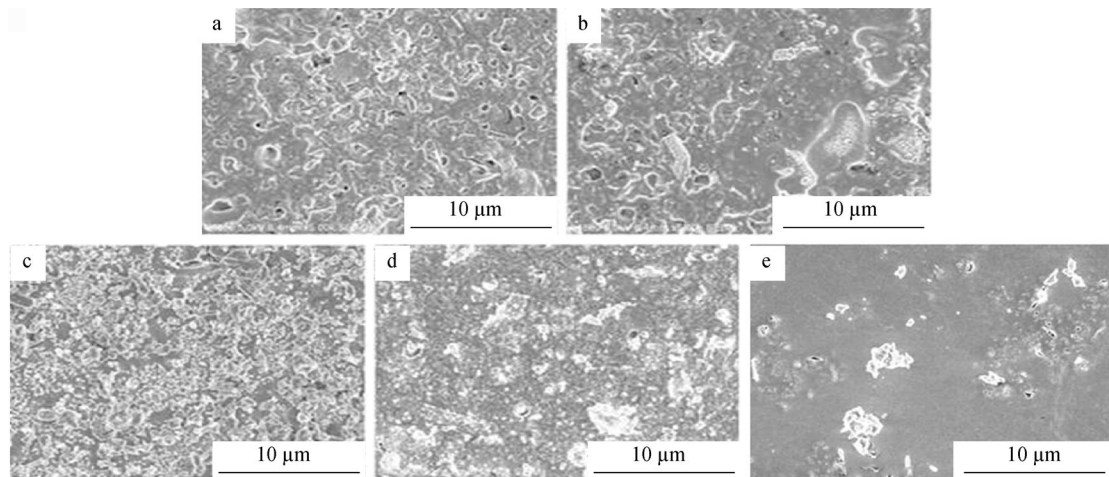


Fig. 3 SEM images of CZTSSe films annealed at **a** 350 °C, **b** 400 °C, **c** 450 °C, **d** 500 °C and **e** 550 °C

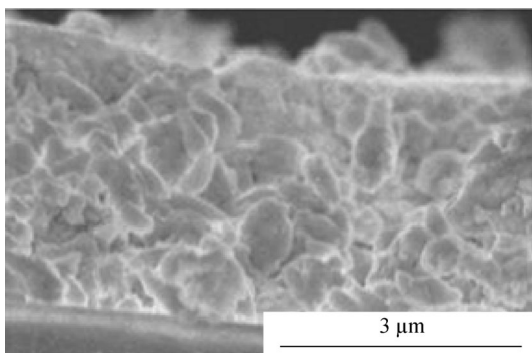


Fig. 4 Cross-sectional SEM image of CZTSSe films annealed at 500 °C

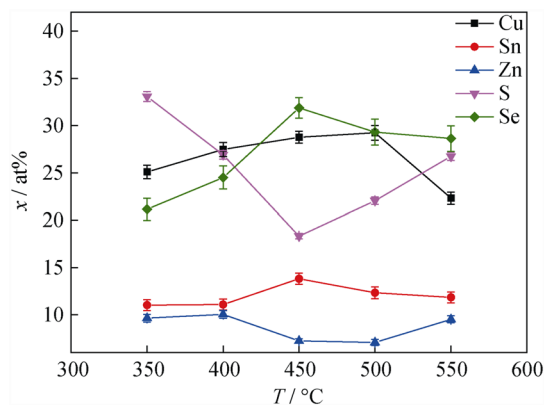


Fig. 5 Relationship between elemental composition and post-annealing temperature of CZTSSe films

the surface SEM image of the CZTSSe films exhibits a few adverse cracks and pinholes to the solar cell performances. The CZTSSe film annealed at 500 °C shows good structure and large grain size (Fig. 4), suggesting that annealing

temperature of 500 °C is a more appropriate sintering temperature in this experiment. Moreover, the $\text{Cu}/(\text{Zn} + \text{S})$, Zn/Sn and $(\text{S} + \text{Se})/(\text{Cu} + \text{Zn} + \text{Sn})$ atomic ratios for the film annealed at 500 °C are 0.96, 0.51 and 1.01, respectively. According to the data in Table 1, the film has poor Cu and rich Sn compositions. The elemental compositions are close to the ideal stoichiometry. These characteristics are helpful for improving the efficiency of solar cells.

3.5 Optical properties

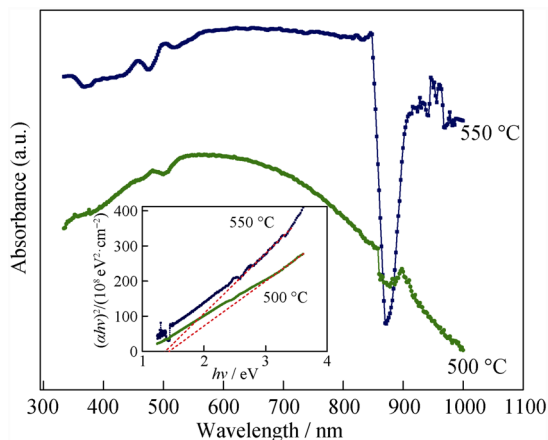
Figure 6 shows the room-temperature UV–Vis absorption spectra of CZTSSe film annealed at 500 and 550 °C. The films show strong optical absorption from visible to near IR region, and its optical absorption coefficient is as high as $1 \times 10^4 \text{ cm}^{-1}$, which is in good agreement with other reports [15, 16]. The optical band gap (E_g) determined from the $(\alpha h\nu)^2$ versus $h\nu$ plots (where α is optical absorption coefficient, $h\nu$ is the photon energy) is 1.37 and 1.44 eV at 500 and 550 °C, respectively, which are close to reported values [17, 18]. This indicates that CZTSSe films obtained using one-pot oleylamine solvothermal synthetic route also have good optical properties.

4 Conclusion

A simple and convenient one-pot oleylamine solvothermal synthetic method for the preparation of CZTS nanoparticles is presented. The prepared CZTS nanocrystals have tetragonal crystallographic structure, as shown by TEM and XRD analysis. The CZTSSe films, prepared by CZTS nanocrystals annealed at 500 °C for 20 min, have kesterite crystal structure with a smooth, uniform and crack-free

Table 1 Atomic ratios of elemental composition of CZTSSe films annealed at 350–550 °C

Annealing temperature/°C	Compositional ratio		
	Cu/(Zn + Sn)	Zn/Sn	(S + Se)/(Cu + Zn + Sn)
350	0.82	0.70	0.99
400	0.88	0.71	0.97
450	0.86	0.38	0.93
500	0.96	0.51	1.01
550	0.72	0.66	1.11

**Fig. 6** Typical room-temperature UV–Vis absorption spectra of CZTSSe films. Inset being plots of $(\alpha h\nu)^2$ versus $h\nu$ for CZTSSe films

topography, strong optical absorption characteristics ($>1 \times 10^4 \text{ cm}^{-1}$), and an ideal optical band gap (1.44 eV). The results indicate that one-pot oleylamine solvothermal synthesis is a facile, cost effective and promising way to synthesize absorber layer for the solar cell applications.

Acknowledgments This study was financially supported by the National Natural Science Foundation of China (Nos. 11564027 and 51262020) and the Scientific Research Foundation of the Higher Education Institutions of Inner Mongolia Autonomous Region of China (No. NJZY16379).

References

- Guo Q, Hillhouse HW, Agrawal R. Synthesis of $\text{Cu}_2\text{ZnSnS}_4$ nanocrystal ink and its use for solar cells. *J Am Chem Soc.* 2009; 131(33):11672.
- Wang J, Xin X, Lin Z. $\text{Cu}_2\text{ZnSnS}_4$ nanocrystals and graphene quantum dots for photovoltaics. *Nanoscale.* 2009;3(8):3040.
- Katagiri H, Jimbo K, Yamada S, Kamimra T, Maw WS, Fukano T, Ito T, Motohiro T. Enhanced conversion efficiencies of $\text{Cu}_2\text{ZnSnS}_4$ -based thin film solar cells by using preferential etching technique. *Appl Phys Exp.* 2008;1(4):041201.
- Guo Q, Grayson MF, Yang WC, Walker BC. Fabrication of 7.2 % efficient CZTSSe solar cells using czts nanocrystals. *J Am Chem Soc.* 2010;132(49):17384.
- Repins I, Beall C, Vora N, DeHart C, Kuciauskas D, Dippo P, To B, Mann J, Hsu W, Goodrich A, Noufi R. Co-evaporated $\text{Cu}_2\text{ZnSnSe}_4$ films and devices. *Sol Energy Mater Sol Cells.* 2012; 101:154.
- Wang W, Winkler MT, Gunawan O, Gokman T, Todorov TK, Zhu Y, Mitzi DB. Device characteristics of CZTSSe thin-film solar cells with 12.6 % efficiency. *Adv Energy Mater.* 2014; 4(7):1301465.
- Seol JS, Lee SY, Lee JC, Nam HD, Kim KH. Electrical and optical properties of $\text{Cu}_2\text{ZnSnS}_4$ thin films prepared by rf magnetron sputtering process. *Sol Energy Mater Sol Cells.* 2003; 75(1–2):155.
- Jimbo K, Kimura R, Kaminura T, Yamada S, Maw WS, Araki H, Oishi K, Katagiri H. $\text{Cu}_2\text{ZnSnS}_4$ -type thin film solar cells using abundant materials. *Thin Solid Films.* 2007;515(15):5997.
- Htay MT, Hashimoto Y, Momose N, Sasaki K, Ishiguchi H, Igarashi S, Sakurai K, Ito K. A cadmium-free $\text{Cu}_2\text{ZnSnS}_4/\text{ZnO}$ heterojunction solar cell prepared by practicable processes. *Jpn J Appl Phys.* 2011;50(3):032301.
- Chalopathy RBV, Jung GS, Ahn BT. Fabrication of $\text{Cu}_2\text{ZnSnS}_4$ films by sulfurization of Cu/ZnSn/Cu pprecursor layers in sulfur atmosphere for solar cells. *Sol Energy Mater Sol Cells.* 2011; 95(12):3216.
- Aaron D, Barkhouse R, Gunawan O, Gokmen T, Todorov TK, Mitzi DB. Device characteristics of a 10.1 % hydrazine-processed $\text{Cu}_2\text{ZnSn}(\text{Se},\text{S})_4$ solar cell. *Prog Photovolt Res Appl.* 2012;20(1):6.
- Guo Q, Kim SJ, Kar M, Shafarman WN, Birkmire W, Stach EA, Agrawal R, Hillhouse HW. Development of CuInSe_2 nanocrystal and nanoring inks for low-cost solar cells. *Nano Lett.* 2008;8(9):2982.
- Wang CZ, Zhu CJ, Zhang TW. Preparation and characterization of $\text{Cu}_2\text{ZnSn}(\text{S}, \text{Se})_4$ thin film as photovoltaic absorber material for solar cells. *Mater Lett.* 2013;108:62.
- Wang CZ, Zhu CJ, Zhang TW, Jian L. $\text{CuIn}(\text{S}, \text{Se})_2$ thin films prepared by selenization and sulfurization of sputtered Cu–In precursors. *Vacuum.* 2013;92:7.
- Pawar SM, Pawar BS, Moholkar AV, Choi DS, Yun JH, Moom JH, Kolekar SS, Kim JH. Single step electrosynthesis of $\text{Cu}_2\text{ZnSnS}_4$ (CZTS) thin films for solar cell application. *Electrochim Acta.* 2010;55(12):4057.
- Zhou YL, Zhou WH, Du YF, Li M, Wu SX. Sphere-like kesterite $\text{Cu}_2\text{ZnSnS}_4$ nanoparticles synthesized by a facile solvothermal method. *Mater Lett.* 2011;65(11):1535.
- Ito K, Nakazawa T. Electrical and optical properties of stannite-type quaternary semiconductor thin films. *Jpn J Appl Phys.* 1988;27(11):2094.
- Katagiri H. $\text{Cu}_2\text{ZnSnS}_4$ thin film solar cells. *Thin Solid Films.* 2005;480–481:426.